

PEGylation of Anti-Sialoadhesin Monoclonal Antibodies Enhances Their Inhibitory Potencies without Impairing Endocytosis in Mouse Peritoneal Macrophages

Julie Ducreux, Donatienne Tyteca, Bernard Ucakar, Thierry Medts, Paul R. Crocker, Pierre J. Courtoy, and Rita Vanbever

Bioconjugate Chem., **2009**, 20 (2), 295-303 • DOI: 10.1021/bc800390g • Publication Date (Web): 14 January 2009

Downloaded from <http://pubs.acs.org> on March 2, 2009

More About This Article

Additional resources and features associated with this article are available within the HTML version:

- Supporting Information
- Access to high resolution figures
- Links to articles and content related to this article
- Copyright permission to reproduce figures and/or text from this article

[View the Full Text HTML](#)

PEGylation of Anti-Sialoadhesin Monoclonal Antibodies Enhances Their Inhibitory Potencies without Impairing Endocytosis in Mouse Peritoneal Macrophages

Julie Ducreux,[†] Donatienne Tyteca,[‡] Bernard Ucakar,[†] Thierry Medts,[‡] Paul R. Crocker,[§] Pierre J. Courtoy,[‡] and Rita Vanbever^{*†}

Department of Pharmaceutical Technology, School of Pharmacy, and Cell Biology Unit, de Duve Institute, Université catholique de Louvain, 1200 Brussels, Belgium, and Wellcome Trust Biocentre, College of Life Sciences, University of Dundee, Dundee DD1 5EH, United Kingdom. Received September 12, 2008; Revised Manuscript Received December 4, 2008

Poly(ethylene glycol) (PEG) 5 kDa and 20 kDa have been previously conjugated to two anti-sialoadhesin (Sn) monoclonal antibodies (mAbs), SER-4 and 3D6, and shown to dramatically increase their inhibitory potency in solid-phase red blood cell binding assays. In the present study, we evaluated the effect of anti-Sn SER-4 and 3D6 mAbs PEGylation on their inhibition of cell adhesion in mouse peritoneal macrophages. We also examined whether Sn-mediated PEGylation could affect plasma membrane functions of macrophages as to prevent accessibility, binding, and endocytosis of macromolecules and particles. Conjugation of PEG to plasma membrane is known to cause immune tolerance by impairing protein–protein and cell–cell interactions. PEGylation of SER-4 and 3D6 mAbs increased by 4-fold their inhibition of Sn-mediated erythrocyte binding to macrophages. PEGylated SER-4 and 3D6 mAbs did not impair macrophage membrane integrity, cell metabolism, nor pinocytosis of macromolecules and phagocytosis of latex particles. Thus, PEGylation of antibodies directed to cell surface receptors could be potentially exploited in a therapeutic setting to increase inhibitory potency of antibodies without impairing vital functions of cells.

INTRODUCTION

The covalent coupling of poly(ethylene glycol) (PEG) to proteins is a well-established technique to enhance the therapeutic potential of peptides and proteins. Multiple benefits of PEGylation include prolongation of protein half-life in the body and elimination of its immunogenicity (for reviews, see *refs 1, 2*). PEGylation has also been extended to cells and tissues. Red blood cells (RBC) were the first example of cell surface PEGylation to produce transfusable universal blood (*3*). The covalent coupling of PEG (molecular weight, MW, 5 kDa) to proteins exposed on RBC surfaces could attenuate the immunologic recognition of surface antigens without adversely affecting viability, morphology, deformability, and other membrane functions (*4, 3*). Interestingly, PEGylation of proteins exposed on the surface of rat pancreatic islets (PEG MW, 5 kDa) conferred immunotolerance of the islets without interfering with glucose homeostasis and islet viability *in vitro* (*5*). *In vivo*, the PEGylation of the islets extended their survival despite a reduced dose of immunosuppressive medication (*6*). The immunoprotective effect of PEG was mainly due to the large steric exclusion volume provided by the flexibility of PEG molecules.

In a recent study, we explored an additional benefit of PEGylation based on the concept of PEG-dependent steric hindrance. We showed that PEGylation of two monoclonal antibodies (mAbs), SER-4 and 3D6, directed to the macrophage adhesion molecule, sialoadhesin (Sn), dramatically increased their efficacy for blocking Sn-mediated interactions (*7*). Sn (Siglec-1, CD169) is a 185 kDa macrophage-restricted adhesion

molecule and a member of the Siglec family of sialic acid binding immunoglobulin (Ig)-like lectins (*8*). Sn mediates sialic acid-dependent adhesion of macrophages to a range of cell types including lymphoid and myeloid cells (*9*). Sn was originally characterized in the mouse as a nonphagocytic sialic acid-dependent sheep erythrocyte receptor expressed on macrophage subsets (*10*), especially those in secondary lymphoid organs (*11*). Sn can be upregulated on monocytes and macrophages during inflammatory responses, including autoimmune diseases (*12, 13*), and on macrophages that infiltrate human breast tumors (*14*). The inhibitory potencies of PEGylated mAbs were evaluated using a well-defined solid-phase RBC binding assay in which recombinant Sn was coated on a plate and allowed to bind RBC in the presence and absence of anti-Sn mAbs. In this assay, neither unconjugated SER-4 nor 3D6 mAb was able to inhibit RBC binding to Sn when added alone, whereas both mAbs were originally identified as blocking antibodies for RBC binding to peritoneal macrophages (*15*). These contradictory results might be explained by the density of Sn coated on the microplate versus that expressed on macrophages. Considering that the interaction of Sn with sialoglycoconjugates is multivalent, the large amount of Sn coated on the plate generated a higher-order multivalency with sialoglycoconjugates on RBC surfaces (*16, 17*). Therefore, the high-density coating of Sn used in the solid-phase RBC binding assay led to higher avidity binding of RBC, which were less efficiently inhibited by SER-4 or 3D6.

The present study aimed to evaluate the inhibitory potency of PEGylated SER-4 and 3D6 in a cellular environment using peritoneal macrophages induced to express Sn (*18*). As PEGylation of cells, such as RBC, and pancreatic islets were shown to camouflage their surface and repel the binding of immune cells and proteins, we also tested the specificity of the inhibition, that is, we evaluated if Sn PEGylation, using PEGylated SER-4 and 3D6, only affected Sn-mediated macrophage interactions or led to Sn receptor-independent side effects, as to prevent the

* Author to whom correspondence should be addressed. Tel.: +32 2 764 73 25. Fax: +32 2 764 73 98. E-mail: rita.vanbever@uclouvain.be.

[†] School of Pharmacy, Université catholique de Louvain.

[‡] de Duve Institute, Université catholique de Louvain.

[§] Wellcome Trust Biocentre.

Table 1. Assessment of Cell Integrity^a

treatment (10 μ g/mL)	cell viability tests		
	Trypan blue exclusion (% of viable cells)	LDH release (% of total)	MTT conversion (% of untreated cells)
untreated cells (control)	92.1 \pm 7.3	13.3 \pm 2.8	100 \pm 11.6
SER-4 and 3D6	89.9 \pm 4.2	13.0 \pm 4.9	108.1 \pm 19.4
SER-4-2PEG 20 kDa	84.5 \pm 3.9	15.3 \pm 4.0	90.0 \pm 11.3
3D6-2PEG 5 kDa	88.0 \pm 1.9	14.2 \pm 3.6	89.3 \pm 4.4
3D6-1PEG 20 kDa	87.6 \pm 2.8	14.7 \pm 4.2	93.5 \pm 13.0
3D6-2PEG 20 kDa	90.0 \pm 3.6	14.7 \pm 2.6	87.0 \pm 17.4
SER-4-2PEG 20 kDa and 3D6-2PEG 20 kDa	92.1 \pm 3.6	13.7 \pm 4.6	89.2 \pm 14.7
Triton 1% (cell death by necrosis)	0.7 \pm 1.3 ^b	98.9 \pm 3.3 ^b	17.9 \pm 2.2 ^b

^a Plasma membrane integrity and cell metabolism of Sn-expressing TPM were assessed by LDH release, Trypan blue exclusion, and MTT reduction. Data are the mean \pm SD of 3 pooled independent experiments (carried out in duplicate). ^b Tukey test, $p < 0.0001$.

accessibility, binding, and endocytosis of macromolecules and particles by macrophages.

EXPERIMENTAL PROCEDURE

Animals. Female C57BL6 mice were bred at the Faculty of Medicine animal facilities of the Université catholique de Louvain (Belgium) and used between 7 and 11 weeks of age. Animals had free access to tap water and laboratory diet during the experimental period. All experimental protocols with mice were approved by the Institutional Animal Care and Use Committee of the Faculty of Medicine of the Université catholique de Louvain.

Preparation of Sn-Expressing Peritoneal Macrophages. Thioglycollate-elicited peritoneal macrophages (TPM) from female C57BL6 mice were obtained 4 days after intraperitoneal injection of 1 mL Brewer's modified thioglycollate broth. About 15 million cells per mouse were recovered by peritoneal lavage with 5 mL HBSS of which $\sim 70\%$ are macrophages (19). TPM were seeded at 1.25×10^6 macrophages/cm² on collagen I precoated multiwell tissue culture plate (Corning Life Sciences, Lowell, MA, USA) in RPMI 1640 supplemented with 2 mM L-glutamine and 10% fetal bovine serum. Nonadherent cells were removed by washing after 40 min of incubation in a humidified atmosphere at 37 °C in 5% CO₂. In order to induce sialoadhesin expression, TPM were incubated in fresh medium supplemented with 2 mM L-glutamine and 10% C57BL6 mouse serum during 3 days (18).

PEGylation of SER-4 and 3D6 mAbs. The most amine reactive groups of SER-4 and 3D6 mAbs were conjugated to 1 or 2 molecules of PEG 5 kDa or 20 kDa, as previously described (7). Modification of mAb with PEG molecules was abbreviated; for example, SER-4-2PEG 5 kDa and denotes a modification of SER-4 mAb with 2 linear PEG chains of 5 kDa.

Evaluation of Cell Membrane Integrity and Cell Metabolism. After 3 days in culture with mouse serum, Sn-expressing TPM were washed with RPMI + 0.1% BSA and precooled at 4 °C. Fc γ receptors on TPM surfaces were blocked using a rat monoclonal antibody against mouse CD16/32 receptors (clone 2.4G2, 1:150) at 4 °C for 20 min. Cells were then incubated with fresh serum-free medium containing 10 μ g/mL of SER-4-2PEG 20 kDa, 3D6-2PEG 5 kDa, 3D6-1PEG 20 kDa, 3D6-2PEG 20 kDa, or a combination of SER-4-2PEG 20 kDa and 3D6-2PEG 20 kDa at 4 °C for 45 min. Cells were finally transferred in a humidified atmosphere at 37 °C in 5% CO₂ during 4 h. Plasma membrane integrity of cells after incubation with PEGylated mAbs was assessed by the release of lactate dehydrogenase (LDH) and the exclusion of Trypan blue. LDH activity was assessed by measuring the NADH consumption during the reduction of pyruvate into lactate (20). Results were expressed as the percentage of activity detected in the medium over the sum of the activities in the medium and in the cells. Trypan blue exclusion results were expressed

as the percentage of viable cells. Cell metabolism was assessed by the reduction of 3-(4,5-dimethylthiazol-2-yl)-2,5-diphenyl tetrazolium bromide (MTT), a yellow water-soluble tetrazolium dye reduced by metabolically active cells to a water-insoluble purple formazan (21). Results were expressed as the percentage of metabolically active cells. In all assays, untreated cells and Triton-treated cells were used as controls.

Red Blood Cell Rosetting Assay. 5×10^4 TPM were added in wells of a collagen I precoated 48-well tissue culture plate and induced to express Sn by culture in 10% mouse serum for 3 days. Cells were washed with RPMI + 0.1% BSA and precooled at 4 °C. Fc γ receptors on TPM surface were blocked, as described above, at 4 °C for 20 min. Cells were then incubated with 300 μ L of 3-fold serial dilutions of the different species of SER-4-PEG or 3D6-PEG alone or in combination at 4 °C for 45 min. Three hundred microliters of freshly prepared human RBC at 1% vol/vol was added directly to the wells and incubated at 37 °C for 30 min. Unbound RBC were removed by repeated washing with medium. The percentage of macrophage binding of >4 RBC, i.e., rosettes, was determined under optical microscopy (100 cells counted; Axiovert S100, Zeiss, Minneapolis, MN, USA) (22). The percentage of rosettes was normalized to the percentage of rosetting activity in the absence of mAbs (considered to be equal to 100%). As controls, TPM were incubated with an irrelevant rat IgG2a, to test the specificity of mAbs, or with nonfunctional PEG in RPMI + 0.1% BSA, to evaluate a possible nonspecific effect of the polymer on RBC binding. In the latter case, the concentration of PEG solution was adjusted to the number of PEG molecules found in a solution composed of a mixture of both PEGylated mAbs.

Characterization of Endocytosis Modes. *Nonspecific Adsorptive Endocytosis.* FITC-albumin was used as tracer of nonspecific adsorptive endocytosis (23). Sn-expressing TPM were first washed with warm medium without serum and incubated at 37 °C during 30 min. The uptake of FITC-albumin by Sn-expressing TPM was measured using increasing concentrations of FITC-albumin in serum-free medium at 37 °C for 2 h. After 6 washes for 30 s with PBS-Ca²⁺-Mg²⁺ (removing 75–80% of tracers bound at 4 °C), intracellular uptake of FITC-albumin was measured in cell lysates prepared in 0.05% (vol/vol) Triton X-100 by fluorimetry (λ_{exc} 485 nm, λ_{em} 530 nm; Packard Fluorocount Microplate Fluorometer, Packard Instrument Company, Meriden, CT, USA). For competition studies, fresh serum-free medium containing 700 μ M bovine albumin (A4378, Sigma-Aldrich, St Louis, MO, USA) was incubated with Sn-expressing TPM 1 h at 4 °C prior to a coinubation with 7 μ M FITC-albumin at 37 °C for 2 h. Cells were then washed 6 times with PBS-Ca²⁺-Mg²⁺ and digested with 0.05% (vol/vol) Triton X-100. Energy depletion of Sn-expressing TPM was performed by incubation with 5 mM sodium azide (NaN₃) and 60 mM 2-deoxy-D-glucose (2-DOG) in serum-free medium (ATP depletion medium). Cells were preincubated in ATP

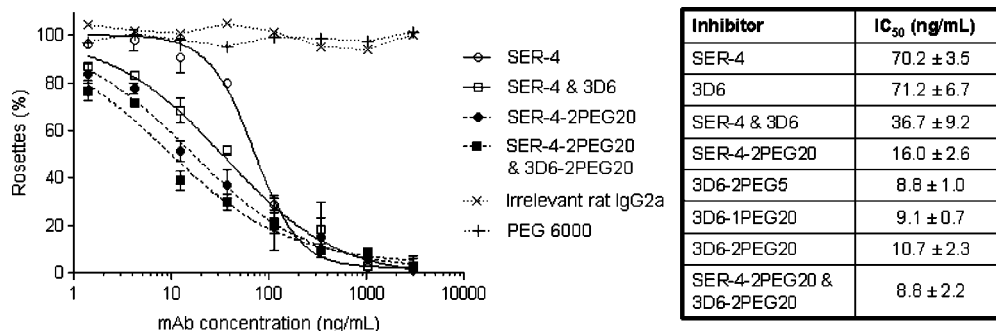


Figure 1. Inhibition of RBC binding to Sn-expressing TPM by PEGylated SER-4 and 3D6 mAbs. Data are the mean \pm SD of two pooled independent experiments (carried out in duplicate). Rosette formation is the % of macrophages that bound >4 RBC. IC₅₀ are concentrations inhibiting 50% of rosette formation. Experiments with irrelevant IgG2a and PEG 6 kDa used in comparable concentrations did not show any inhibitory effect on rosette formation.

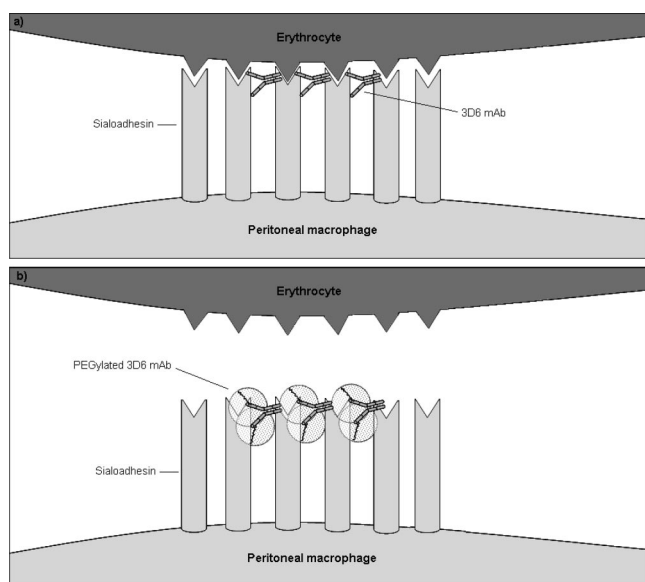


Figure 2. Creation of a sterical hindrance by PEG on Sn molecules. Interaction of an erythrocyte and a macrophage occurs when both sialic acids and Sn cluster, to create high-avidity binding. At the same concentration, unmodified 3D6 mAb did not inhibit erythrocyte binding to the macrophage (a), whereas PEGylated 3D6 mAb did (b). The higher potency of PEGylated mAbs to inhibit erythrocyte binding was likely due to a sterical effect created by PEG molecules around Sn.

depletion medium at 37 °C for 20 min and incubated with 7 μ M FITC-albumin in ATP depletion medium for 2 additional hours. Cells were then washed 6 times with PBS-Ca²⁺-Mg²⁺ and digested with 0.05% (vol/vol) Triton X-100.

Receptor-Mediated Endocytosis. Iron-saturated transferrin was labeled with ¹²⁵I using iodogen-precoated tubes to a specific radioactivity of 2600–3300 cpm/ng protein. Sn-expressing TPM surface binding of ¹²⁵I-transferrin was determined by incubating cells pre-cooled at 4 °C with increasing concentrations of ¹²⁵I-transferrin in serum-free medium supplemented with 0.1% BSA for 1 h. Cells were then washed and radioactivity was measured in cell lysates prepared in 0.05% (vol/vol) Triton X-100 (Minaxi γ gamma counter, Packard Instrument Company, Meriden, CT, USA). For competition studies, human serum was incubated with Sn-expressing TPM 1 h at 4 °C prior to a coinubation with 50 nM ¹²⁵I-transferrin for one additional hour at 4 °C. Cells were then washed 6 times with PBS-Ca²⁺-Mg²⁺ and surface-digested with 0.2% (wt/vol) Pronase in RPMI at 4 °C for 45 min to distinguish transferrin accessible on the plasma membrane (Pronase-sensitive) from sequestered transferrin (Pronase-resistant) (24). Pronase-resistant fraction (containing intracellular ¹²⁵I-transferrin) was pelleted by centrifugation at

250 \times g at 4 °C for 5 min. The supernatant (containing surface-accessible transferrin) was kept, and the pellet was finally washed twice with PBS-Ca²⁺-Mg²⁺ and lysed in 0.05% (vol/vol) Triton X-100. Radioactivity was measured in Pronase-resistant and Pronase-sensitive fractions. Energy depletion of Sn-expressing TPM was performed by incubation in ATP depletion medium at 37 °C for 20 min (see above). Cells were then pre-cooled at 4 °C and incubated with 50 nM ¹²⁵I-transferrin in ATP depletion medium for 1 h. Cells were washed and reincubated at 37 °C in fresh pre-warmed ATP depletion medium for 10 min. Cells were then rapidly cooled down to 4 °C, washed 6 times with PBS-Ca²⁺-Mg²⁺, surface digested, and radioactivity in Pronase-resistant and Pronase-sensitive fractions were measured.

Internalisation Assays. Sn-expressing TPM were first washed with warm medium without serum and incubated at 37 °C over 30 min. Cells were washed and pre-cooled at 4 °C. Fc γ receptors on TPM surface were blocked as described above at 4 °C for 20 min. Cells were finally washed and incubated with a combination of SER-4–2PEG 20 kDa and 3D6–2PEG 20 kDa at 4 °C for 45 min prior to incubation with tracers of endocytosis.

FITC-Albumin Endocytosis. FITC-albumin was directly added to cells at a final concentration of 7 μ M and incubated at 37 °C for the indicated intervals. Cells were washed 6 times with PBS-Ca²⁺-Mg²⁺, and intracellular uptake of FITC-albumin was measured on sonicated cell lysates prepared in 0.05% (vol/vol) Triton X-100 by fluorimetry.

¹²⁵I-Transferrin Endocytosis. ¹²⁵I-transferrin was directly added to cells at a final concentration of 50 nM and allowed to bind at 4 °C for 1 h. Cells were washed 6 times at 4 °C with PBS-Ca²⁺-Mg²⁺ and reincubated at 37 °C in fresh pre-warmed serum-free medium supplemented with 0.1% BSA for the indicated intervals. Cells were then rapidly cooled down to 4 °C, washed, and surface-digested with 0.2% (wt/vol) Pronase in RPMI at 4 °C for 45 min. Radioactivity was measured in Pronase-resistant and Pronase-sensitive fractions to distinguish intracellular from surface-accessible transferrin.

Phagocytosis. Red fluorescent carboxylate-modified latex beads of 2 μ m were used as tracer of phagocytosis. Following the incubation with PEGylated mAbs, an equivalent volume of latex beads in serum-free medium was added directly to the wells at a final concentration of 270 beads/nL, mixed, and incubated at 37 °C for the indicated intervals. After 6 washes for 30 s with PBS-Ca²⁺-Mg²⁺ (removing more than 80% of the beads bound at 4 °C), uptake of the beads was measured on sonicated cell lysates prepared in 0.05% (vol/vol) Triton X-100 by fluorimetry (λ_{exc} 485 nm, λ_{em} 610 nm). To inhibit phagocytosis (25), Sn-expressing TPM were first preincubated with 10 μ M cytochalasin B in serum-free medium at 37 °C for 30 min

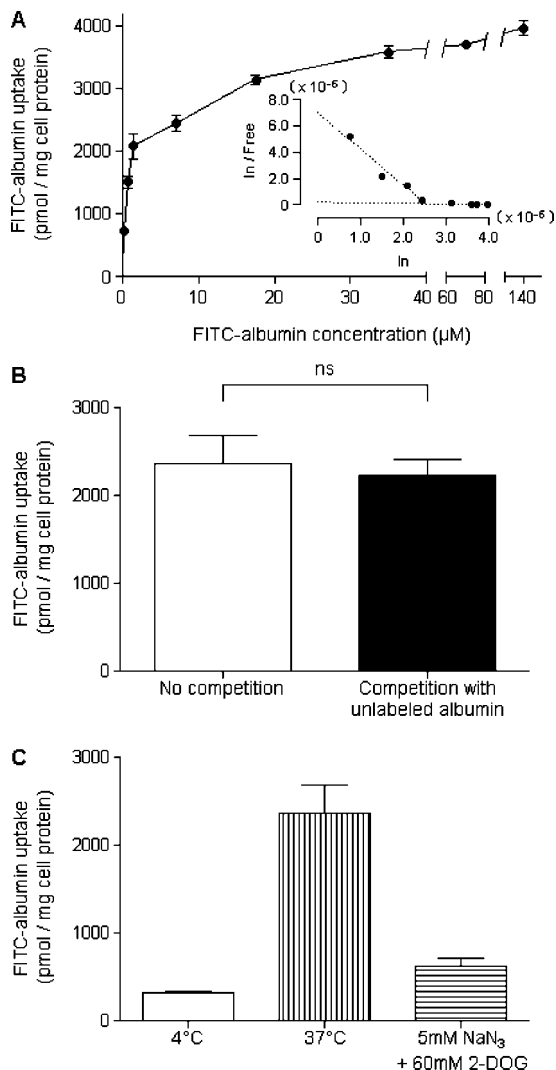


Figure 3. FITC-albumin is taken up by nonspecific adsorptive endocytosis in Sn-expressing TPM. (A) Adsorptive uptake of FITC-albumin. FITC-albumin uptake was measured as a function of substrate concentration in untreated cells at 37 °C for 2 h. Inset, scatchard analysis of the uptake (In values in abscissa are in $\mu\text{mol}/\mu\text{g}$ cell protein; In/Free ratios in the ordinate are in $\text{L}/\mu\text{g}$ cell protein). Two components of internalization were revealed with a high internalization constant ($K_{\text{uptake}} = 0.36 \mu\text{M}$) for the first one and a low internalization constant for the second one ($K_{\text{uptake}} = 18.88 \mu\text{M}$). (B) No competition for FITC-albumin uptake at 37 °C for 2 h. Cells were incubated with 7 μM FITC-albumin alone (open bar) or with a 100-fold excess of unlabeled albumin (filled bar); ns: no significant difference (*t* test, $p > 0.05$). (C) Endocytic uptake of FITC-albumin is evidenced by inhibition at low temperature and upon energy depletion. Cells were incubated with 7 μM FITC-albumin at 4 °C for 1 h (open bar) or at 37 °C for 2 h (vertically striped bar). Cellular ATP was depleted by incubating cells in ATP depletion medium at 37 °C for 20 min. Cells were then incubated with 7 μM FITC-albumin in ATP depletion medium at 37 °C for 2 h (horizontally striped bar).

and incubated with latex beads (270 particles/nL) in serum-free medium containing 10 μM cytochalasin B at 37 °C for the indicated intervals. Cells were then washed 6 times 30 s with PBS- Ca^{2+} - Mg^{2+} and digested with 0.05% (vol/vol) Triton X-100.

Localization of Fluorescent Latex Beads in Sn-Expressing TPM by Confocal Microscopy. Untreated and PEGylated cells, that is, pretreated with the combination of SER-4–2PEG 20 kDa and 3D6–2PEG 20 kDa, were incubated with 1 μm green-fluorescent latex beads or 2 μm red-fluorescent latex beads at 37 °C for 3 h, washed 6 times 30 s with PBS- Ca^{2+} - Mg^{2+} , and were fixed at room temperature in 4% paraformaldehyde for

30 min. Cells were then washed 5 times with PBS and aspecific sites were blocked by incubation in BSA/lysine solution at room temperature for 30 min. To label the surface membrane of Sn-expressing TPM, rat antimouse F4/80 mAb (1:200) was incubated in BSA/lysine solution at room temperature for 1 h. Cells were then washed 6 times 5 min with BSA/lysine and incubated with Alexafluor 647-conjugated goat antirat IgG antibody (1:200) at room temperature for 1 h. Cells were finally washed 6 times 5 min with PBS, postfixed in 4% paraformaldehyde, washed 3 times with PBS, and mounted on glass slides with mowiol. Cells were observed with a Zeiss confocal laser scanning microscope LSM510 Meta-multiphoton. Data were analyzed with Zeiss LSM software to obtain x - y , x - z , and y - z views of cells.

Fate of Anti-Sn mAbs. 3D6 mAb was labeled with ^{125}I using iodogen-precoated tubes to a specific radioactivity of 2800–3500 cpm/ng of protein. Fc γ receptors on Sn-expressing TPM surface were blocked, and cells were then surface-labeled with 5 $\mu\text{g}/\text{mL}$ ^{125}I -3D6 mAb in serum-free medium supplemented with 0.1% BSA at 4 °C for 45 min. Fresh prewarmed serum-free medium was then directly added to ^{125}I -3D6 solution in wells, and cells were incubated at 37 °C for the indicated intervals. Cells were then rapidly cooled down to 4 °C, washed 6 times with PBS- Ca^{2+} - Mg^{2+} , and surface-digested with 0.2% (wt/vol) Pronase in RPMI for 45 min as described above.

Analysis. All data were normalized to the cell protein content. Protein concentrations were measured by microBCA protein assay using BSA as the protein standard. Unless otherwise stated, results were expressed as mean \pm standard deviation (SD) of 3 wells of 1 representative experiment. Statistical comparisons of experimental values (by unpaired *t* test or one-way analysis of variance (ANOVA) test and Tukey post-test) and other mathematical analyses were performed using the GraphPad Prism software for Windows (v 5.00, La Jolla, CA, USA). Differences were considered significant at $p < 0.05$.

RESULTS AND DISCUSSION

SER-4 and 3D6 are monoclonal rat IgG2a anti-Sn antibodies directed to two distinct epitopes of mouse Sn, domains 2 and/or 3 for SER-4, and domain 1 for 3D6 (9). We showed previously in solid-phase binding assays that PEGylation of SER-4 and 3D6 mAbs strongly promoted their inhibitory potencies against RBC binding (7). SER-4 carrying 2 molecules of PEG 20 kDa (SER-4–2PEG 20 kDa) or 3D6 carrying 2 molecules of PEG 5 kDa (3D6–2PEG 5 kDa) alone each resulted in about 75% inhibition, which was only reached by the combination of unmodified mAbs. Moreover, 3D6 carrying 1 or 2 molecules of PEG 20 kDa (3D6–1PEG 20 kDa or 3D6–2PEG 20 kDa) could totally inhibit RBC binding as shown by serial dilutions. When SER-4-PEG and 3D6-PEG were tested in combination, their inhibitory potency further increased in line with the degree of PEGylation.

In the present study, only these derivatized mAbs and the combination of SER-4 and 3D6 with 2 molecules of 20 kDa were tested. SER-4 and 3D6 mAbs with other extents of derivatization that did not inhibit RBC binding in solid-phase assays were not studied.

Effect of PEGylated Anti-Sn mAbs Binding on Sn-Expressing TPM Viability. PEG molecules larger than 400 Da are considered nontoxic, and PEG has been approved by the FDA for use in food and cosmetics (26). However, Murad et al. showed that, when surface of RBC was highly derivatized with PEG 5 kDa, PEGylation induced adverse structural and functional effects on cells (4). Therefore, in the present assay, we evaluated the effect of PEGylated SER-4 and 3D6 on Sn-expressing TPM viability and cell function using different cytotoxicity assays (Table 1): LDH release and Trypan blue

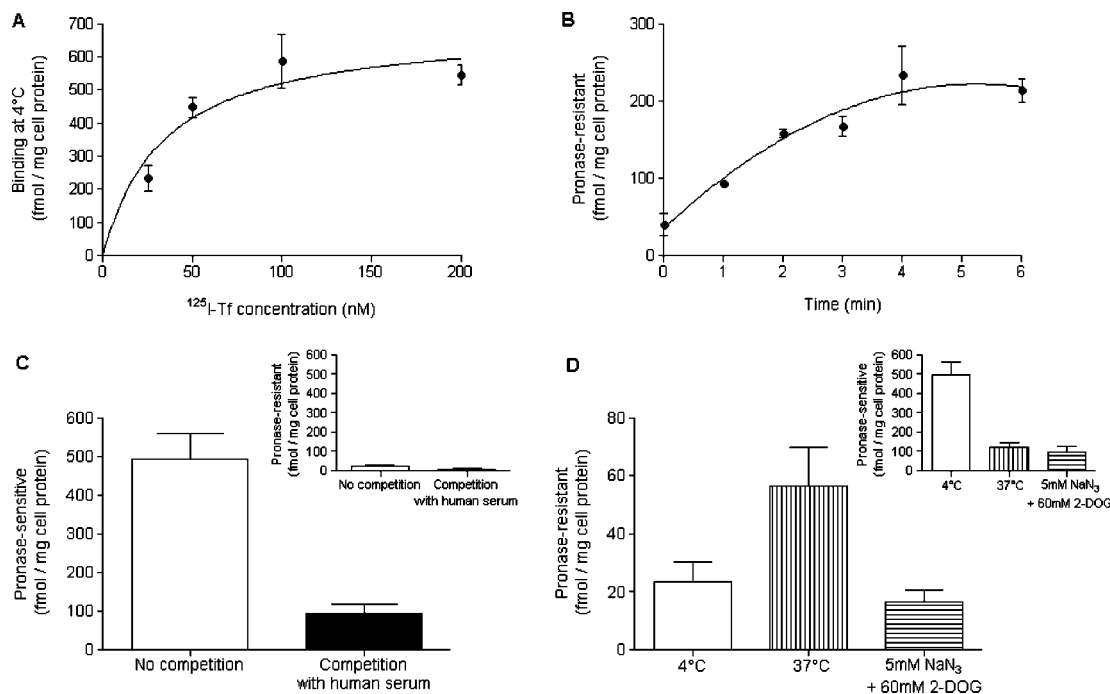


Figure 4. ^{125}I -transferrin endocytosis by Sn-expressing TPM. (A) Specific binding of ^{125}I -transferrin at increasing concentrations at 4 °C. (B) Kinetics of ^{125}I -transferrin internalization. Cells were surface-labeled with 50 nM ^{125}I -transferrin at 4 °C, washed, and reincubated at 37 °C in transferrin-free medium for the indicated intervals. Increase in Pronase-resistant counts indicate values of intracellular transferrin. (C) Competitive binding of ^{125}I -transferrin at 4 °C. Cells were incubated with ^{125}I -transferrin in serum-free medium for 1 h (open bar) or incubated with human serum for 1 h then with ^{125}I -transferrin in human serum for an additional hour (filled bar). Pronase-sensitive counts indicate values of surface-accessible transferrin. Inset, Pronase-resistant counts of the same cells. (D) Endocytosis of ^{125}I -transferrin is evidenced by incubation at low temperature and upon energy depletion. Cells were surface-labeled with 50 nM ^{125}I -transferrin at 4 °C and then washed (open bar) or further reincubated at 37 °C in transferrin-free medium for 10 min (vertically striped bar). ATP-depleted cells were surface-labeled at 4 °C with 50 nM ^{125}I -transferrin in ATP depletion medium for 1 h, washed, and reincubated at 37 °C in ATP depletion conditions for 10 min (horizontally striped bar). Inset, Pronase-sensitive counts of the same cells.

exclusion to assess plasma membrane integrity and MTT reduction to determine the metabolic activity. In these assays and in the subsequent ones, we tested the PEGylated mAbs concentration that inhibited with the highest efficacy the binding of RBC to Sn in solid-phase binding assay (7). Whatever the PEGylated mAbs, none of them showed any appreciable damage to the plasma membrane or alteration of metabolic activity of TPM.

Inhibition of RBC Binding to Sn-Expressing TPM by PEGylated Anti-Sn mAbs. In order to assess the inhibitory potency of PEGylated SER-4 and 3D6 mAbs on Sn-mediated interaction in a cellular environment, we used peritoneal macrophages induced to express Sn. As already shown (22), parent SER-4 and 3D6 mAbs inhibited RBC binding to macrophages with a high efficacy when used alone (Figure 1). However, PEGylated mAbs used alone were all better inhibitors than unconjugated SER-4 or 3D6 mAbs used alone or in combination. On the basis of IC_{50} , SER-4 containing 2 molecules of PEG 20 kDa was a 4-fold stronger inhibitor than unlabeled SER-4. The combination of SER-4 and 3D6, each carrying 2 molecules of PEG 20 kDa resulted in an IC_{50} of ~ 9 ng/mL, a 4-fold reduction IC_{50} as compared to the mixture of the non-PEGylated mAbs. This suggested that PEG molecules conferred an additional sterical hindrance around the antibody and, hence, around the receptor that prevented with higher efficacy the RBC approach (as illustrated in Figure 2). To verify that the decreased RBC binding was not the result of a nonspecific interaction of PEG molecules with macrophage surfaces, RBC binding to TPM was evaluated after incubation with PEG alone (Figure 1). PEG was not able to inhibit RBC binding by itself, indicating that the increased inhibitory potency provided by PEGylated mAbs was not due to a nonspecific binding of the polymer to the macrophage surface. Because it was the most efficient, further

studies were carried out with the combination of SER-4 and 3D6 coupled with 2 molecules of PEG 20 kDa.

Effect of Sn-Mediated PEGylation of Macrophages on Albumin and Transferrin Endocytosis. Scott et al. have shown that, when erythrocytes are PEGylated, the rapid motility and molecular flexibility of the heavily hydrated PEG chains affect the global surface of cells and prevent protein–protein interactions as antibody-mediated RBC agglutination via blood group antigen (27). Therefore, PEGylation of Sn-expressing TPM with PEGylated SER-4 and 3D6 mAbs could affect the entire cell surface and thereby impair endocytosis mechanisms of macrophages, one of their key functions. This was examined by a series of endocytosis assays.

Nonspecific Adsorptive Endocytosis of Albumin by Sn-Expressing TPM. Nonspecific adsorptive endocytosis is a saturable process at high concentration involving, prior to internalization, interaction with nonspecific sites on the plasma membrane. In contrast to kidney proximal tubules or endothelial cells, albumin is internalized in macrophages by nonspecific interaction (23) and is accepted as a tracer of nonspecific adsorptive endocytosis in this cell type (28). To characterize the nonspecific adsorptive endocytosis of albumin in Sn-expressing TPM, its uptake was investigated in various conditions (Figure 3). FITC-albumin uptake was measured as a function of substrate concentration in untreated cells. Figure 3A shows saturation of uptake at a concentration of $17.5 \mu\text{M}$ indicating that FITC-albumin is internalized via a process saturable at high concentration, characteristic of adsorptive endocytosis. The efficiency of accumulation after 2 h was estimated at about 150×10^6 molecules per cell, i.e., 2 orders of magnitude higher than fluid-phase endocytosis. Subsequent studies were carried out at a nonsaturating albumin concentration ($7 \mu\text{M}$). To further clarify whether the binding of FITC-albumin

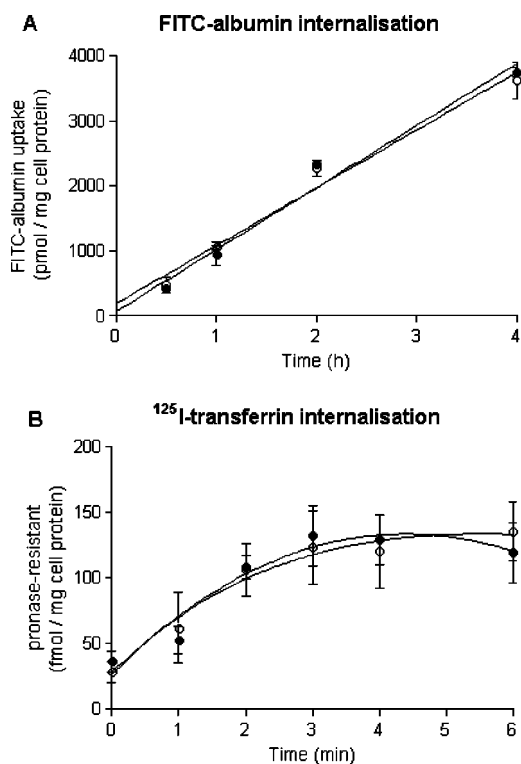


Figure 5. Effect of PEGylated anti-Sn mAbs on nonspecific adsorptive endocytosis of FITC-albumin (A) and on receptor-mediated endocytosis of ^{125}I -transferrin (B) in Sn-expressing TPM. Cells were either left untreated (open circles) or pretreated with a combination of SER-4–2PEG20 and 3D6–2PEG20 both at $10\ \mu\text{g}/\text{mL}$ (filled circles) at $4\ ^\circ\text{C}$ for 45 min. (A) FITC-albumin was added at a final concentration of $7\ \mu\text{M}$ and cells were reincubated at $37\ ^\circ\text{C}$ for the indicated intervals. Experiments were reproduced twice with similar results. (B) After incubation with $50\ \text{nM}$ ^{125}I -transferrin at $4\ ^\circ\text{C}$ for 1 h, cells were reincubated at $37\ ^\circ\text{C}$ in transferrin-free medium for the indicated intervals. Increase of Pronase-resistant counts indicate the amounts of intracellular transferrin. Experiments were reproduced three times with similar results.

to Sn-expressing TPM was specific or not, a competition study was carried out using a 100-fold excess of unlabeled albumin (Figure 3B). Unlabeled albumin did not affect the uptake of FITC-albumin, indicating that this tracer binds nonspecifically to Sn-expressing TPM surface. To confirm that FITC-albumin was taken up by endocytosis, we looked at the effect of low temperature and energy depletion. Figure 3C shows that both treatments dramatically reduced the uptake of FITC-albumin in macrophages. Taken together, these results confirm that TPM induced to express Sn internalize albumin by nonspecific adsorptive endocytosis.

Receptor-Mediated Endocytosis of Transferrin by Sn-Expressing TPM. Receptor-mediated endocytosis is a specific adsorptive endocytosis mode characterized by the specific binding of a ligand to its cell surface receptor followed by internalization of ligand–receptor complexes. Transferrin is the most commonly used tracer of receptor-mediated endocytosis, and its internalization was at first studied in peritoneal macrophages induced to express Sn (Figure 4). As shown in Figure 4A, ^{125}I -transferrin binding at $4\ ^\circ\text{C}$ to untreated TPM reached saturation at $\sim 600\ \text{fmol}/\text{mg}$ cell protein, corresponding to $\sim 35\ 000$ binding sites/cell, with an apparent K_d of $30\ \text{nM}$. Further studies were carried out with an initial concentration of $50\ \text{nM}$ ^{125}I -transferrin (below saturation). Pronase-resistant or intracellular transferrin increased very rapidly (~ 3500 molecules/cell/min) to level off after ~ 6 min (Figure 4B), a time sufficient for apotransferrin–receptor complexes to be recycled on the cell surface (29). In a competition study, human

serum (containing $35\ \mu\text{M}$ transferrin) significantly decreased the binding of ^{125}I -transferrin to the cell surface, indicating that this tracer specifically binds to Sn-expressing TPM in a receptor-dependent manner (Figure 4C, Pronase-sensitive fraction). As expected for endocytosis, acquisition of intracellular ^{125}I -transferrin was largely inhibited at $4\ ^\circ\text{C}$ (Figure 4D). Since formation of clathrin-coated pits and -vesicles supporting receptor internalization requires cellular ATP, receptor-mediated endocytosis is an energy-dependent process (30). Cellular ATP of Sn-expressing TPM was depleted, and ^{125}I -transferrin internalization was studied for 10 min. Figure 4D shows that ATP depletion significantly reduced the uptake of ^{125}I -transferrin in macrophages. Cellular ATP depletion also reduced the binding of ^{125}I -transferrin (Figure 4D, inset), as ATP is also needed for the recycling of transferrin receptors (31). These results indicate that TPM induced to express Sn internalize transferrin via receptor-mediated endocytosis.

Effect of PEGylated Anti-Sn mAbs on Nonspecific Adsorptive Endocytosis of Albumin and Receptor-Mediated Endocytosis of Transferrin. To assess the effect of PEGylated anti-Sn mAbs on FITC-albumin and ^{125}I -transferrin uptake in Sn-expressing TPM, the combination of SER-4–2PEG20 kDa and 3D6–2PEG 20 kDa mAbs was incubated with cells at $4\ ^\circ\text{C}$ prior to addition of $7\ \mu\text{M}$ FITC-albumin or $50\ \text{nM}$ ^{125}I -transferrin. PEGylation of Sn-expressing TPM using PEGylated SER-4 and 3D6 impaired neither the binding nor the kinetics of internalization of either FITC-albumin or ^{125}I -transferrin at any time (Figure 5). Uptake of FITC-albumin (Figure 5A) and intracellular accumulation of ^{125}I -transferrin into cells (Figure 5B) were comparable in PEGylated and untreated TPM. PEGylation of Sn expressed on the TPM surface using PEGylated mAbs inhibited neither nonspecific adsorptive nor specific receptor-mediated protein interactions, and this might be explained in two ways. First, as Jang et al. showed that surface PEGylation of pancreatic islets could not completely prevent the infiltration of cytotoxic molecules into the islets (32), we suggest that PEG molecules coupled to antibodies directed to Sn on the TPM surface did not prevent the passage of macromolecules, such as albumin and transferrin, across the meshes of PEG. Second, it remains possible that the specific and local PEGylation of Sn expressed on TPM surface using PEGylated mAbs had no steric impact on the whole cell surface and therefore did not prevent the approach, the binding and the internalization of albumin and transferrin (as illustrated in Figure 6). Indeed, the studies on pancreatic islets showed that an efficient immunocamouflage of cells by PEG is in part governed by the surface concentration of PEG (33): the higher the cell surface covered by PEG molecules, the higher the PEG hindrance.

Effect of Sn-Mediated PEGylation of Macrophages on Phagocytosis of Latex Beads. Phagocytosis is a receptor- and actin-dependent process utilized by mononuclear phagocytes and neutrophils to ingest and clear large particles ($>0.5\ \mu\text{m}$) (34). This internalization process serves to remove foreign particles such as parasites or to remove host cells such as apoptotic bodies (35). Scott et al. showed that PEGylation of sheep erythrocytes could inhibit their phagocytosis without impairing protein interactions such as antibody-mediated agglutination via blood group antigen (27). Therefore, although PEGylation of Sn expressed on the TPM surface did not affect the internalization of macromolecules such as albumin and transferrin, it could negatively affect phagocytosis of particles. In comparison with macromolecules, particles of larger size could not easily escape the steric effect created by PEG molecules on the cell surface.

Phagocytosis of Latex Beads by Sn-Expressing TPM. The effect of PEGylation of TPM surface on phagocytosis was investigated by studying the accumulation of red fluorescent

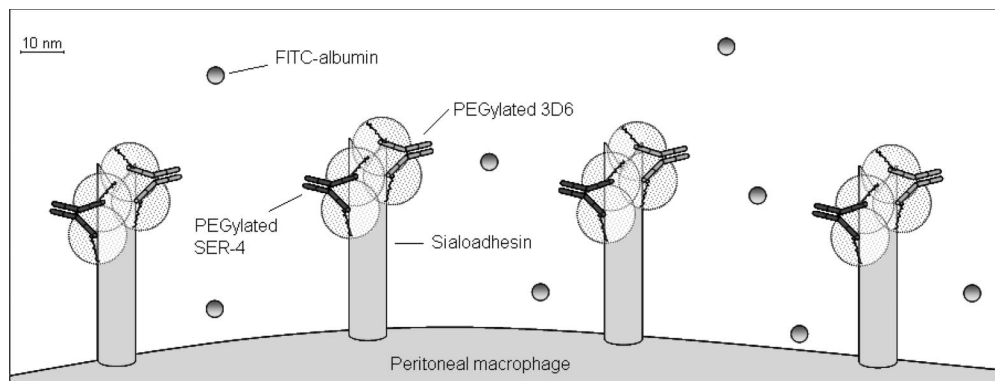


Figure 6. SER-4 and 3D6 mAbs modified with 2 molecules of PEG 20 kDa did not inhibit protein interactions with Sn expressing macrophages. The specific and local PEGylation of Sn expressed on macrophage surface using PEGylated SER-4 and 3D6 mAbs had no steric impact on the whole cell surface and therefore did not prevent the approach, the binding and the internalization of albumin. The number of Sn molecules per cell was estimated from the number of ^{125}I -3D6 mAbs bound per cell (see Figure 10), and Sn molecules were homogenously distributed on the macrophage surface.

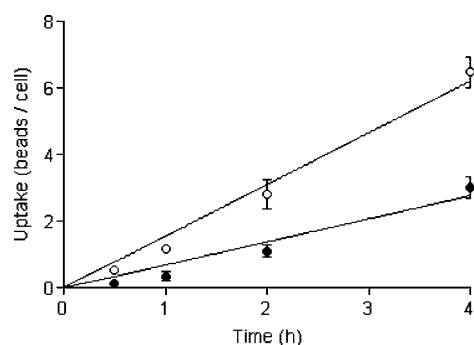


Figure 7. Inhibition of $2\ \mu\text{m}$ red fluorescent latex beads phagocytosis in Sn-expressing TPM by $10\ \mu\text{M}$ cytochalasin B. Sn-expressing TPM were either left untreated (open circles) or preincubated with $10\ \mu\text{M}$ cytochalasin B at $37\ ^\circ\text{C}$ for 30 min (filled circles). A final concentration of 270 beads/nL was added and cells were reincubated at $37\ ^\circ\text{C}$ for the indicated intervals.

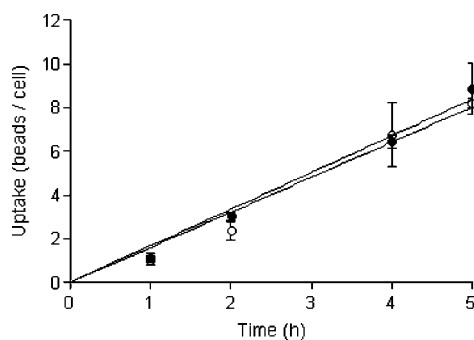


Figure 8. Effect of PEGylated anti-Sn mAbs on phagocytosis of $2\ \mu\text{m}$ red fluorescent latex beads in Sn-expressing TPM. Cells were either left untreated (open circles) or pretreated with a combination of SER-4-2PEG20 and 3D6-2PEG20 both at $10\ \mu\text{g}/\text{mL}$ (filled circles) at $4\ ^\circ\text{C}$ for 45 min. A final concentration of 270 beads/nL was added, and cells were reincubated at $37\ ^\circ\text{C}$ for the indicated intervals. Experiments were reproduced three times with similar results.

carboxylate-modified polystyrene latex beads of a large size ($2\ \mu\text{m}$, 270 particles/nL). Latex beads can be taken up by both pinocytosis and phagocytosis, but the relative contribution of phagocytosis increases with the particle diameter (25). Figure 7 shows that $2\text{-}\mu\text{m}$ -diameter latex beads were largely internalized by phagocytosis, as suggested by a $\sim 50\%$ inhibition by cytochalasin B, an inhibitor of microfilaments formation during phagocytosis (36).

Effect of PEGylated Anti-Sn Mabs on Phagocytosis of Latex Beads. To assess the effect of PEGylation of Sn-

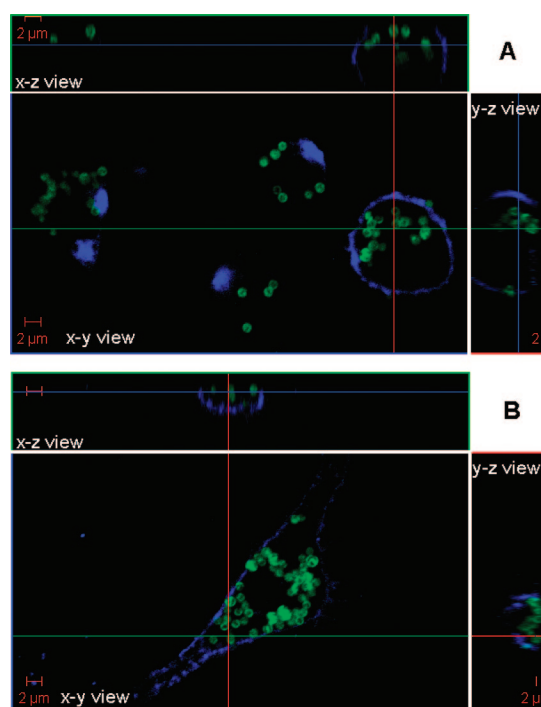


Figure 9. Effect of PEGylated anti-Sn mAbs on phagocytosis of latex beads in Sn-expressing TPM: localization of latex beads in untreated (A) and PEGylated (B) macrophages. After incubation with $1\ \mu\text{m}$ latex beads (green; 270 beads/nL) for 3 h, cells were fixed and incubated with rat antimouse F4/80 mAb, then with Alexafluor 647-conjugated goat antirat IgG antibody to identify the plasma membrane (blue).

expressing TPM on phagocytosis, the combination of SER-4-2PEG 20 kDa and 3D6-2PEG 20 kDa mAbs was first incubated with cells at $4\ ^\circ\text{C}$ prior to addition of latex beads at a final concentration of 270 particles/nL. Figure 8 shows that PEGylation of Sn on TPM did not detectably interfere with phagocytosis. The rate of accumulation of the beads was constant and identical in PEGylated cells as compared with untreated cells. Internalization of latex beads by both untreated and PEGylated cells was confirmed by confocal microscopy. Internalization of $1\ \mu\text{m}$ latex beads was observed into both untreated (Figure 9A) and PEGylated cells (Figure 9B) by reference to the plasma membrane that was immunolabeled in blue using anti-F4/80 mAb. The same observations were made with $2\ \mu\text{m}$ latex beads (data not shown).

These results suggest that PEGylation of Sn expressed on the TPM surface using PEGylated mAbs only hindered the

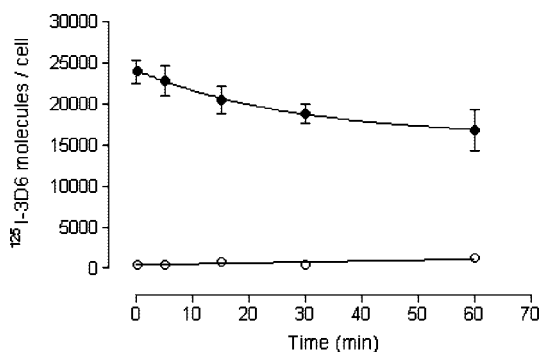


Figure 10. Fate of ^{125}I -3D6 mAb in Sn-expressing TPM. Cells were surface-labeled with $5\ \mu\text{g}/\text{mL}$ ^{125}I -3D6 mAb at $4\ ^\circ\text{C}$ for 45 min. Fresh, prewarmed serum-free medium was then directly added to ^{125}I -3D6 solution in wells, and cells were incubated at $37\ ^\circ\text{C}$ for the indicated intervals. Intracellular 3D6 mAb molecules (open circles) were distinguished from surface-accessible 3D6 mAb molecules (filled circles) by digestion of cell surface with 0.2% (wt/vol) Pronase.

receptor and its environment. Consequently, the PEG hindrance did not affect the whole cell surface and did not impair the binding and uptake of particles.

Fate of ^{125}I -Anti-Sn mAb in Sn-Expressing TPM. Our present study shows that Sn-mediated PEGylation of macrophages improves the inhibition of cell adhesion activity of Sn without affecting pinocytosis of macromolecules and phagocytosis of particles. To verify that the absence of effect on endocytosis and phagocytosis was not due to a shedding of PEGylated mAbs from the cell surface, we studied the fate of ^{125}I -3D6 mAb in Sn-expressing cells (Figure 10). ^{125}I -3D6 mAb was not detectably internalized when cells were incubated at $37\ ^\circ\text{C}$ (Figure 10, open circles, Pronase-resistant counts), and shedding of ^{125}I -3D6 mAb bound to the cell surface was moderate (Figure 10, Pronase-sensitive counts) over 1 h. Binding of ^{125}I -3D6 mAb at $4\ ^\circ\text{C}$ to Sn-expressing TPM reached $400\ \text{fmol}/\text{mg}$ cell protein, corresponding to $\sim 24\ 000$ molecules/cell. A slight release of ^{125}I -3D6 mAb was observed during the first 15 min at $37\ ^\circ\text{C}$ (~ 230 molecules/cell/min), decreasing the number of binding sites to $\sim 20\ 000$ molecules/cell. Then, an equilibrium between bound mAbs and free mAbs in solution kept the binding of ^{125}I -3D6 mAb to Sn-expressing cell surface almost constant over 1 h. The release of mAbs from the cell surface slowed down to ~ 80 molecules/cell/min, and $\sim 17\ 000$ molecules of ^{125}I -3D6 mAb remained bound to the cell surface after 1 h at $37\ ^\circ\text{C}$ (Figure 10, filled circles, Pronase-sensitive counts).

In conclusion, this study reports that PEGylation of SER-4 and 3D6 mAbs directed to the macrophage adhesion molecule, Sn, greatly increases their efficacy to inhibit RBC Sn-mediated binding to macrophages as compared with unmodified mAbs. Flexibility and motility of PEG molecules on SER-4 and 3D6 mAbs most likely create a steric hindrance around antibodies that increases the inhibition of RBC specific binding to Sn. Moreover, we show that a local Sn-mediated PEGylation of macrophages and the consequent steric effects of PEG are safe to cells, as PEGylated SER-4 and 3D6 mAbs did not impair membrane integrity, cell metabolism nor the pinocytosis of macromolecules and the phagocytosis of particles close to the size of bacteria. Thus, PEGylation of antibodies directed to cell surface receptors could be potentially exploited in a therapeutic setting, such as autoimmune or inflammatory diseases, to increase the inhibitory potency of antibodies without impairing vital cell functions.

ACKNOWLEDGMENT

This work was supported by a FIRST EUROPE EPH3310300R054F/415744 grant (Région Wallonne, Belgium,

and European social fund). The authors would like to thank the Fonds de la Recherche Scientifique - Fonds National de la Recherche Scientifique (F.R.S-FNRS, Belgium) and the Région Bruxelloise (confocal microscopy). Rita Vanbever is a Chercheur Qualifié of the FNRS.

LITERATURE CITED

- (1) Veronese, F. M., and Pasut, G. (2005) PEGylation, successful approach to drug delivery. *Drug Discovery Today* 10, 1451–1458.
- (2) Chapman, A. P. (2002) PEGylated antibodies and antibody fragments for improved therapy: a review. *Adv. Drug Delivery Rev.* 54, 531–545.
- (3) Tan, Y., Qiu, Y., Xu, H., Ji, S., Li, S., Gong, F., and Zhang, Y. (2006) Decreased immunorejection in unmatched blood transfusions by attachment of methoxypolyethylene glycol on human red blood cells and the effect on D antigen. *Transfusion* 46, 2122–2127.
- (4) Murad, K. L., Mahany, K. L., Brugnara, C., Kuypers, F. A., Eaton, J. W., and Scott, M. D. (1999) Structural and functional consequences of antigenic modulation of red blood cells with methoxypoly(ethylene glycol). *Blood* 93, 2121–2127.
- (5) Lee, D. Y., Yang, K., Lee, S., Chae, S. Y., Kim, K. W., Lee, M. K., Han, D. J., and Byun, Y. (2002) Optimization of monomethoxy-polyethylene glycol grafting on the pancreatic islet capsules. *J. Biomed. Mater. Res.* 62, 372–377.
- (6) Lee, D. Y., Park, S. J., Nam, J. H., and Byun, Y. (2006) A combination therapy of PEGylation and immunosuppressive agent for successful islet transplantation. *J. Controlled Release* 110, 290–295.
- (7) Ducreux, J., Vanbever, R., and Crocker, P. R. (2008) The inhibitory potencies of monoclonal antibodies to the macrophage adhesion molecule sialoadhesin are greatly increased following PEGylation. *Bioconjugate Chem.* 19, 2088–2094.
- (8) Crocker, P. R., Mucklow, S., Bouckson, V., McWilliam, A., Willis, A. C., Gordon, S., Milon, G., Kelm, S., and Bradfield, P. (1994) Sialoadhesin, a macrophage sialic acid binding receptor for haemopoietic cells with 17 immunoglobulin-like domains. *EMBO J.* 13, 4490–4503.
- (9) van den Berg, T. K., Breve, J. J., Damoiseaux, J. G., Dopp, E. A., Kelm, S., Crocker, P. R., Dijkstra, C. D., and Kraal, G. (1992) Sialoadhesin on macrophages: its identification as a lymphocyte adhesion molecule. *J. Exp. Med.* 176, 647–655.
- (10) Crocker, P. R., and Gordon, S. (1986) Properties and distribution of a lectin-like hemagglutinin differentially expressed by murine stromal tissue macrophages. *J. Exp. Med.* 164, 1862–1875.
- (11) Schadee-Eestermans, I. L., Hoefsmit, E. C., van de Ende, M., Crocker, P. R., van den Berg, T. K., and Dijkstra, C. D. (2000) Ultrastructural localisation of sialoadhesin (siglec-1) on macrophages in rodent lymphoid tissues. *Immunobiology* 202, 309–325.
- (12) Hartnell, A., Steel, J., Turley, H., Jones, M., Jackson, D. G., and Crocker, P. R. (2001) Characterization of human sialoadhesin, a sialic acid binding receptor expressed by resident and inflammatory macrophage populations. *Blood* 97, 288–296.
- (13) Jiang, H. R., Hwenda, L., Makinen, K., Oetke, C., Crocker, P. R., and Forrester, J. V. (2006) Sialoadhesin promotes the inflammatory response in experimental autoimmune uveoretinitis. *J. Immunol.* 177, 2258–2264.
- (14) Nath, D., Hartnell, A., Happerfield, L., Miles, D. W., Burchell, J., Taylor-Papadimitriou, J., and Crocker, P. R. (1999) Macrophage-tumour cell interactions: identification of MUC1 on breast cancer cells as a potential counter-receptor for the macrophage-restricted receptor, sialoadhesin. *Immunology* 98, 213–219.
- (15) Crocker, P. R., Kelm, S., Dubois, C., Martin, B., McWilliam, A. S., Shotton, D. M., Paulson, J. C., and Gordon, S. (1991) Purification and properties of sialoadhesin, a sialic acid-binding receptor of murine tissue macrophages. *EMBO J.* 10, 1661–1669.

- (16) Crocker, P. R., Werb, Z., Gordon, S., and Bainton, D. F. (1990) Ultrastructural localization of a macrophage-restricted sialic acid binding hemagglutinin, SER, in macrophage-hematopoietic cell clusters. *Blood* 76, 1131–1138.
- (17) Hashimoto, Y., Suzuki, M., Crocker, P. R., and Suzuki, A. (1998) A streptavidin-based neoglycoprotein carrying more than 140 GT1b oligosaccharides: Quantitative estimation of the binding specificity of murine sialoadhesin expressed on CHO cells. *J. Biochem.* 123, 468–478.
- (18) Crocker, P. R., Hill, M., and Gordon, S. (1988) Regulation of a murine macrophage haemagglutinin (sheep erythrocyte receptor) by a species-restricted serum factor. *Immunology* 65, 515–522.
- (19) Wu, Q., Feng, Y., Yang, Y., Jingliu, Zhou, W., He, P., Zhou, R., Li, X., and Zou, J. (2004) Kinetics of the phenotype and function of murine peritoneal macrophages following acute inflammation. *Cell Mol. Immunol.* 1, 57–62.
- (20) Vassault, A. (1983) *Lactate Dehydrogenase. UV-method with pyruvate and NADH. Methods of enzymatic analysis*, pp 118–125, VCH, New York.
- (21) Weyermann, J., Lochmann, D., and Zimmer, A. (2005) A practical note on the use of cytotoxicity assays. *Int. J. Pharm.* 288, 369–376.
- (22) Crocker, P. R., and Gordon, S. (1989) Mouse macrophage hemagglutinin (sheep erythrocyte receptor) with specificity for sialylated glycoconjugates characterized by a monoclonal antibody. *J. Exp. Med.* 169, 1333–1346.
- (23) Kooistra, T., Pratten, M. K., and Lloyd, J. B. (1981) Serum-dependence of fluid-phase pinocytosis and specificity in adsorptive pinocytosis of simple proteins in rat peritoneal macrophages. *Biosci. Rep.* 1, 587–594.
- (24) Cupers, P., Veithen, A., Kiss, A., Baudhuin, P., and Courtoy, P. J. (1994) Clathrin polymerization is not required for bulk-phase endocytosis in rat fetal fibroblasts. *J. Cell Biol.* 127, 725–735.
- (25) Pratten, M. K., and Lloyd, J. B. (1986) Pinocytosis and phagocytosis: the effect of size of a particulate substrate on its mode of capture by rat peritoneal macrophages cultured in vitro. *Biochim. Biophys. Acta* 881, 307–313.
- (26) Fishburn, C. S. (2008) The pharmacology of PEGylation: Balancing PD with PK to generate novel therapeutics. *J. Pharm. Sci.* 97, 4167–4183.
- (27) Scott, M. D., Murad, K. L., Koumpouras, F., Talbot, M., and Eaton, J. W. (1997) Chemical camouflage of antigenic determinants: Stealth erythrocytes. *Proc. Natl. Acad. Sci. U.S.A.* 94, 7566–7571.
- (28) Faghihi, S. M., Aronson, N. N., Jr., and Dean, R. T. (1982) Temperature dependence of certain integrated membrane functions in macrophages. *J. Cell Sci.* 57, 115–127.
- (29) Mukherjee, S., Ghosh, R. N., and Maxfield, F. R. (1997) Endocytosis. *Physiol. Rev.* 77, 759–803.
- (30) Schmid, S. L., and Carter, L. L. (1990) ATP is required for receptor-mediated endocytosis in intact cells. *J. Cell Biol.* 111, 2307–2318.
- (31) Podbilewicz, B., and Mellman, I. (1990) ATP and cytosol requirements for transferrin recycling in intact and disrupted MDCK cells. *EMBO J.* 9, 3477–3487.
- (32) Jang, J. Y., Lee, D. Y., Park, S. J., and Byun, Y. (2004) Immune reactions of lymphocytes and macrophages against PEG-grafted pancreatic islets. *Biomaterials* 25, 3663–3669.
- (33) Chen, A. M., and Scott, M. D. (2001) Current and future applications of immunological attenuation via pegylation of cells and tissue. *BioDrugs* 15, 833–847.
- (34) Allen, L. A. H., and Aderem, A. (1996) Mechanisms of phagocytosis. *Curr. Opin. Immunol.* 8, 36–40.
- (35) Conner, S. D., and Schmid, S. L. (2003) Regulated portals of entry into the cell. *Nature* 422, 37–44.
- (36) Cooper, J. A. (1987) Effects of cytochalasin and phalloidin on Actin. *J. Cell Biol.* 105, 1473–1478.

BC800390G